organics

MDPI

Communication

Adamantane-Functionalized Phthalimide Scaffold: Pathways to Supramolecular Interactions and Drug Discovery

Hamidou Keita

Department of Chemistry, Clemson University, Clemson, SC 29634, USA; hkeita@g.clemson.edu

Abstract: Herein, the synthesis of a novel adamantanyl-functionalized phthalimide scaffold is demonstrated. The novel compound could be used as a precursor for various synthetic pathways owing to the generic use of adamantane substituents as the driving force for supramolecular interactions with macrocycles and N-substituted phthalimide derivatives as a core structure in numerous drugs. The adamantanyl-functionalized phthalimide scaffold contains bromide groups on the C4 and C5 positions of the benzene ring, effectively allowing further facile modifications of the scaffold. The structure was fully characterized including single-crystal X-ray crystallography. The crystal structure shows an adamantane moiety at an angle of 115.57(7)° to the phthalimide core, hence sterically freeing the adamantane unit for host–guest interactions.

Keywords: adamantane; phthalimides; N-substitution; supramolecular materials; surface recognition; crystal structure; noncovalent; host–guest interactions

check for updates

Citation: Keita, H. Adamantane-Functionalized Phthalimide Scaffold: Pathways to Supramolecular Interactions and Drug Discovery. *Organics* **2021**, *2*, 388–394. https://doi.org/10.3390/org2040022

Academic Editor: Wim Dehaen

Received: 7 September 2021
Accepted: 8 November 2021
Published: 11 November 2021

Publisher's Note: MDPI stays neutral with regard to jurisdictional claims in published maps and institutional affiliations.

Copyright: © 2021 by the author. Licensee MDPI, Basel, Switzerland. This article is an open access article distributed under the terms and conditions of the Creative Commons Attribution (CC BY) license (https://creativecommons.org/licenses/by/4.0/).

1. Introduction

Adamantane is a polycyclic hydrocarbon with fused chair cyclohexane rings with remarkable properties due to its lipophilicity and rigid structure [1]. It was only after Siewerth et al. illustrated a facile synthetic method for adamantane that it received greater attention from the materials and pharmaceutical industries [2,3]. As a result of the sustained interest in adamantane derivatives, amantadine (1-aminoadamantane) became the first derivative to exhibit potent anti-influenza properties and an antiviral activity against rubella viruses [4,5]. Remarkably, research in adamantane-based materials has extended far and wide to areas such as drug delivery [6–9], transitional metal catalysis [10–12], metal–organic frameworks, supramolecular chemistry and surface recognition [13–15].

Due to its rigid structure and high symmetry, the adamantane moiety can form strong and directional supramolecular inclusion complexes with macrocyclic host molecules such as cucurbiturils and cyclodextrins [6,7]. For instance, Kim et al. reported a highly removable homogeneous transition metal catalyst in aqueous media via host–guest interactions between an adamantanyl moiety and β-cyclodextrin [12]. Using modified ligands to retrieve metal catalysts from reaction mixtures has immense industrial applications. The pharmaceutical industries rely on the association equilibrium constant of about $K = 5.2 \times 10^4\ M^{-1}$ of adamantane-β-cyclodextrin complexes to purify products through supramolecular interactions [16].

Given the myriad of applications for adamantanyl-decorated materials in drug design, catalysis, separation and new materials, we report the synthesis and structural analysis of a novel adamantanyl-functionalized phthalimide scaffold, 2-[(adamantan-1-yl)methyl]-5,6-dibromo-1*H*-isoindole-1,3(2*H*)-dione, or **AdBr**. In this work, the structure of **AdBr** was characterized by NMR spectroscopy, FTIR spectroscopy, single-crystal X-ray diffraction and elemental analysis. The **AdBr** scaffold could potentially be modified via Buckwald–Hartwig amination or other synthetic strategies to obtain new materials such as N-heterocyclic compounds [17–19].

2. Materials and Methods

1,2-Dimethyl-4,5-dibromobenzene (**XyBr**) and 4,5-dibromo phthalic acid (**AcidBr**) were synthesized as previously reported [20,21]. All other materials were of reagent quality and of HPLC grade and used as received. ^{1}H and $^{13}C\{^{1}H\}$ NMR spectra were obtained using a Bruker 300 MHz spectrometer. Chemical shifts δ (in ppm) for ^{1}H and ^{13}C NMR were referenced to $SiMe_4$ using the residual protio-solvent as an internal standard. For ^{1}H NMR: $CDCl_3$, 7.26 ppm. For ^{13}C NMR: $CDCl_3$, 77.16 ppm. Coupling constants (*J*) were expressed in hertz (Hz). Infrared spectra were recorded with 1 cm^{-1} resolution on a Shimadzu IRAffinity-1S spectrometer. Elemental analyses were performed at Atlantic Microlab, Inc. (Norcross, GA, USA). All reactions were performed under an inert N_2 atmosphere using standard Schlenk. All subsequent experiments were performed under ambient conditions using standard benchtop techniques.

2.1. Preparation of 4,5-Dibromo Phthalic Acid (AcidBr)

4,5-Dibromo o-xylene 200.00 mg (0.76 mmol) was dispersed in a 3.6 mL pyridine and 6.0 mL water mixture. Then, 473.00 mg $KMnO_4$ (2.99 mmol, 3.95 eq) was added to it and refluxed for 2 h. After, 945.00 mg of KMnO4 was added seven times (6.62 g total), and the reaction was set to continue refluxing overnight. After 16 h, the mixture was filtered while hot, and the residue was washed with hot water. The filtrate was reduced under vacuum to remove the pyridine, and the remaining solution was acidified with conc. HCl to form a white precipitate which was filtered and dried. Yield 208.00 mg, 85%. Due to the limited solubility of the product in the organic solvent, a satisfactory NMR spectrum could not be obtained. ATR-IR: v 3091 (vw), 2904 (vw), 2791 (vw), 2616 (vw), 2516 (vw), 1700 (s), 1515 (w), 1408 (w), 1289 (m), 1239(s), 1158 (w), 1077 (m), 876 (m), 816 (w), 776 (m), 701(w), 607 (vw).

2.2. Preparation of 2-[(Adamantan-1-yl)Methyl]-5,6-Dibromo-1H-Isoindole-1,3(2H)-Dione (AdBr)

4,5-Dibromo phthalic acid **(AcidBr)** 722.00 mg (2.24 mmol) and 1-adamantanemethyl ammonium salt 450.70 mg (2.24 mmol) were placed in 100 mL RBF equipped with a stir bar. Then, 15.0 mL acetic acid was added and refluxed at 120 °C for 16 h. The mixture was allowed to cool to RT, and 10.0 mL of water was added to it. The precipitate formed was filtered and washed with methanol (10 mL × 3) in a centrifuge tube. The precipitate was dried in vacuo to afford a gray solid (650.00 mg, 1.44 mmol, 64%). MP, 245.8–247.0 °C. ^{1}H NMR (300 MHz, $CDCl_3$): δ 8.10 (s, 2H), 3.39 (s, 2H), 1.99 (s, 3H), 1.63–1.54 (m,12H). ^{13}C NMR (300 MHz, $CDCl_3$): δ 167.18, 131.79, 131.27, 128.40, 50.16, 40.79, 36.66, 35.58, 28.21. ATR-IR: v 3089 (vw), 2909 (m), 2840 (w), 1764 (w), 1706 (s), 1355 (s), 1253 (w), 1137 (w), 1088 (m), 990 (m), 903 (w), 856 (m), 743 (s), 611 (m), 581 (s). Anal. Calc. for $C_{19}H_{19}Br_2NO_2$: C, 50.36; H, 4.23; N, 3.09. Found: C, 50.22; H, 4.25; N, 3.08.

2.3. Crystal Structure Data Acquisition

A specimen of $C_{19}H_{19}Br_2NO_2$ (**AdBr**), with approximate dimensions of 0.256 × 0.312 × 0.452 mm, was used for the X-ray crystallographic analysis. The X-ray intensity data were measured. The integration of the data using a triclinic unit cell yielded a total of 40,110 reflections at a maximum θ angle of 33.18° (0.65 Å resolution), of which 6439 were independent (average redundancy 6.229, completeness = 98.7%, R_{int} = 1.69%, R_{sig} = 1.07%), and 6143 (95.40%) were greater than $2\sigma(F^2)$. The final cell constants of $\underline{a}$ = 7.3485(3) Å, $\underline{b}$ = 8.0912(4) Å, $\underline{c}$ = 15.0118(7) Å, α = 100.7690(10)°, β = 102.3410(10)°, γ = 93.5710(10)° and volume = 851.72(7) $Å^3$ are based upon the refinement of the XYZ centroids of reflections above 20 σ(I). The calculated minimum and maximum transmission coefficients (based on crystal size) were 0.7672 and 1.0000.

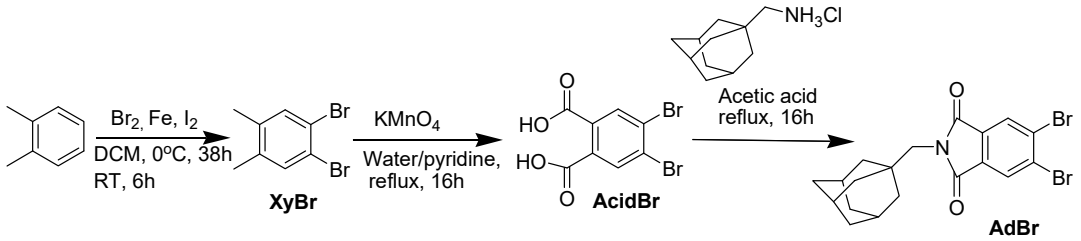
The structure was solved and refined using the Bruker SHELXTL Software Package, using the space group P-1, with Z = 2 for the formula unit, $C_{19}H_{19}Br_2NO_2$. The final anisotropic full-matrix least squares refinement on F^2 with 217 variables converged at R1 = 1.61% for the observed data, and wR2 = 4.13% for all data. The goodness of fit was

1.088. The largest peak in the final difference electron density synthesis was 0.663 $e^-/Å^3$, and the largest hole was −0.346 $e^-/Å^3$, with an RMS deviation of 0.057 $e^-/Å^3$. On the basis of the final model, the calculated density was 1.767 g/cm^3 and F(000), 452 e^-.

3. Results and Discussion

3.1. Synthesis and Spectroscopy

As the first step towards constructing an adamantanyl-functionalized phthalimide scaffold, we pursued the bromination of o-xylene to yield 1,2-dimethyl-4,5-dibromobenzene (**XyBr**) (Scheme 1), as reported [20]. **XyBr** was subsequently oxidized with $KMnO_4$ in the water/pyridine mixture to form the corresponding 4,5-dibromo phthalic acid (**AcidBr)** which could not be characterized with a ^1H NMR spectroscope due to its poor solubility [21]. However, FTIR analysis indicated a very broad trough at 3000 cm^{-1} due to O-H stretching, and a carbonyl peak at 1706 cm^{-1} which proves that the methyl groups are oxidized to carboxylic acids.



Scheme 1. Preparation of 2-[(adamantan-1-yl)methyl]-5,6-dibromo-1*H*-isoindole-1,3(2*H*)-dione (AdBr) with o-xylene as the starting material.

Interestingly, while there are numerous examples of N-substituted phthalimide derivatives due to the role of their structural unit in various drugs [22], examples of 2-[(adamantan-1-yl)methyl]-5,6-dibromo-1*H*-isoindole-1,3(2*H*)-dione (**AdBr**) with a dibromo group are rare [23,24]. As a result, we devised a novel strategy for the straightforward synthesis of an adamantanyl-functionalized phthalimide scaffold which contains bromide groups on the C4 and C5 positions of the benzene ring, effectively allowing further facile modifications of the scaffold. In order to synthesize **AdBr** (Scheme 1), **AcidBr** was reacted with 1-adamantanemethylamine hydrochloride [25] in acetic acid for 16 h under reflux conditions. 1-Adamantanemethylamine was selected because it is less bulky around the amine group compared to 1-adamantaneamine. The methylene spacer in the adamantylmethyl substituent allows host molecules such as β-cyclodextrin to form a supramolecular complex with the adamantanyl moiety with minimal steric interference from the phthalimide core.

After TLC showed completion of the reaction, the desired product was obtained by adding water to the reaction mixture and filtering the precipitate formed, which was a gray solid. However, when recrystallized in a chloroform/pentane mixture, a white crystal was formed. ^1H-NMR showed characteristic adamantane peaks from 1.99 to 1.54 ppm, with the methylene peak resonating at 3.39 ppm as a singlet. In contrast, the methylene peak of 1-adamantanemethylamine hydrochloride showed a quartet at 2.66 ppm [25]. When compared to **XyBr**, the aromatic protons shifted downfield to 8.10 ppm, indicating the successful appendage of 1-adamantanemethylamine (Figure 1).

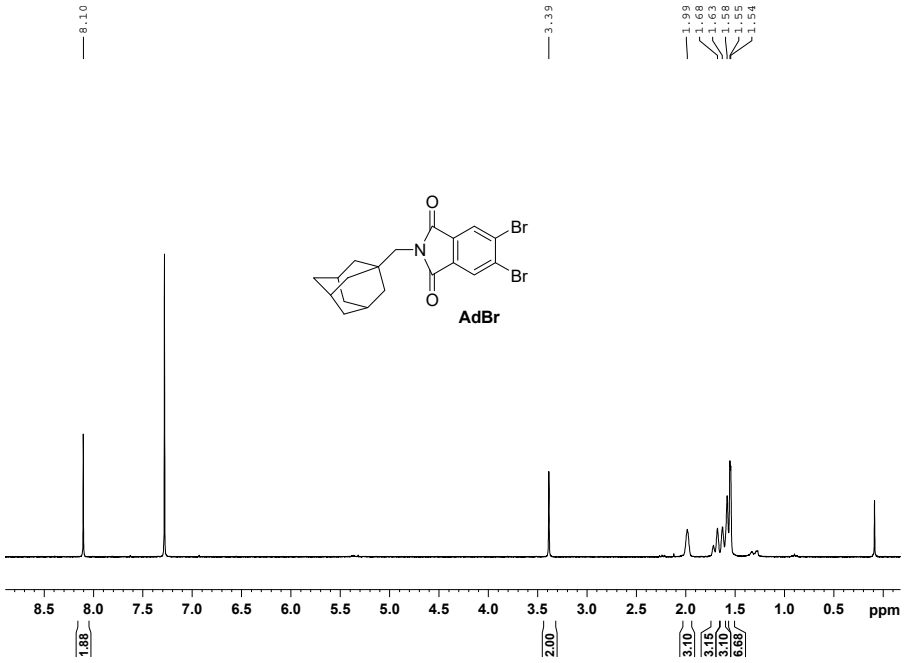


Figure 1. ^{1}H-NMR ($CDCl_3$) spectrum of AdBr.

^{13}C-NMR further proved the synthesis of **AdBr** by showing a characteristic peak of carbonyl carbon at 167.18 ppm and methylene carbon at 50.16 ppm (Figure 2). The FTIR spectrum of **AdBr** (Figure 3) indicated a characteristic carbonyl peak at 1706 cm^{-1} and stronger C-H stretching at 2904 cm^{-1} and 2830 cm^{-1} compared to **XyBr** and **AcidBr**. The stronger C-H stretching in **AdBr** relative to its precursors indicates the successful functionalization with the adamantane moiety which has significant aliphatic C-H bonds.

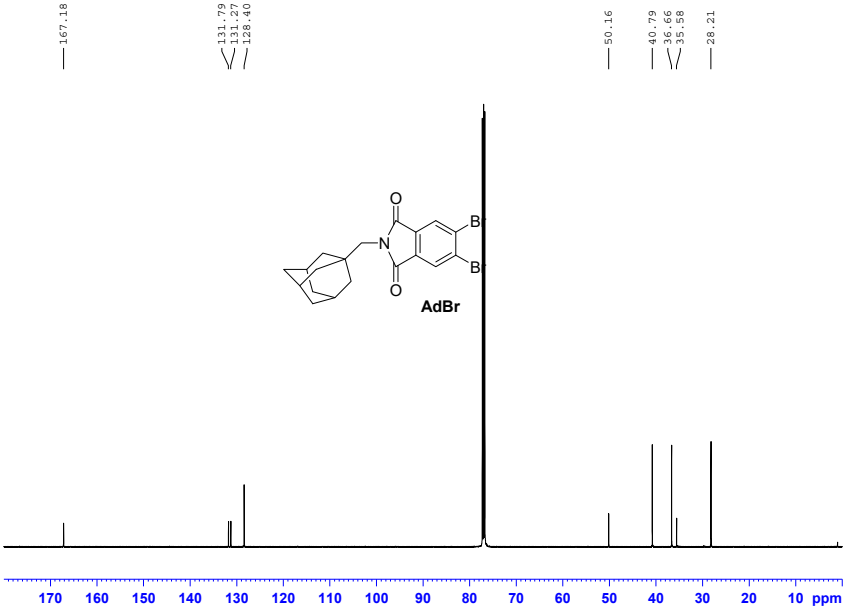


Figure 2. ^{13}C-NMR ($CDCl_3$) spectrum of AdBr.

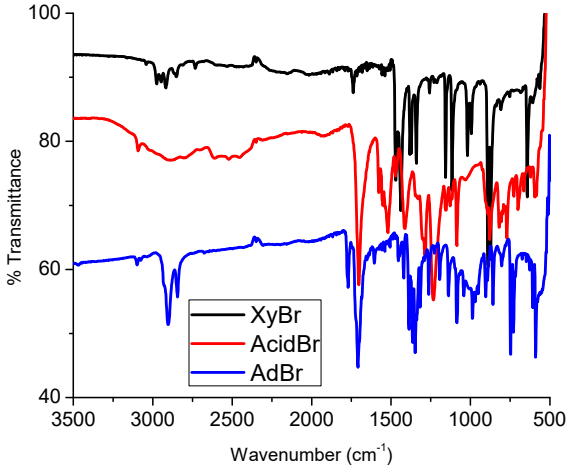
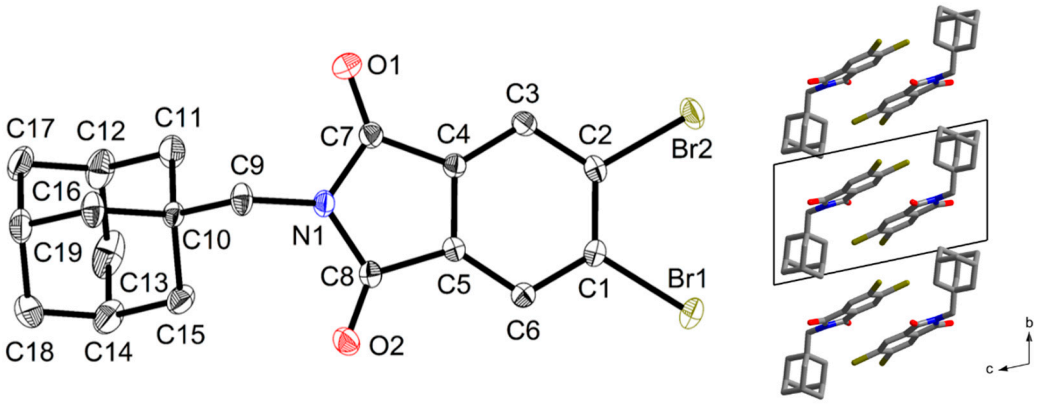


Figure 3. FTIR spectra of AdBr and its precursors.

3.2. Crystallography

Diffraction-quality single crystals of **AdBr** were obtained from a saturated solution of chloroform through gradual diffusion of pentane vapor at room temperature. After 24 h, large white crystals were observed and subjected to crystallographic analysis. The crystal system was determined to be triclinic, and the space group was of the P-1 type. The N1-C9-C10 bond angle was 115.57(7)°, which suggests the adamantane moiety is not in the same plane as the phthalimide unit (see supporting information). The adamantane moiety was almost perpendicular to the phthalimide core, and this observation was also reported by Basaric et al. [24]. The orientation of the adamantanyl unit is suitable for interaction with host macrocycles for formation of an inclusion complex without steric interference from the phthalimide unit (Figure 4). Furthermore, the carbonyl bond distance for O1-C7 was 1.2104(11) Å, which is within the reported range of 1.201–1.235 Å [26–28]. The twinned nature of the AdBr molecule in the unit cell of the crystal structure suggests a Br–Br halogen interaction, which could be the driving force for crystallization [29,30].



(**A**) (**B**)

Figure 4. (**A**) ORTEP diagram of **AdBr**. Thermal ellipsoids are shown at the 50% probability level. Hydrogen atoms have been omitted for the purpose of clarity. Selected distances (Å) and angles (°): Br1-C1, 1.8832(8); Br2-C2, 1.8819(8); O1-C7, 1.2104(11); O2-C8, 1.2107(10); N1-C8, 1.4009(11); N1-C7, 1.4036(11); N1-C9, 1.4629(11); C1-C6, 1.3987(12); C8-N1-C7, 111.55(7); C8-N1-C9, 123.81(7); C7-N1-C9, 123.41(7); C6-C1-C2, 121.28(8); C6-C1-Br1, 117.88(6); C2-C1-Br1, 120.84(6); C3-C2-C1, 121.31(8); C3-C2-Br2, 117.96(6). (**B**) Molecular arrangement in the crystal structure of **AdBr**.

4. Conclusions

The synthesis of a novel adamantanyl-functionalized phthalimide scaffold was demonstrated. The scaffold has bromide groups on the C4 and C5 positions of the benzene ring, effectively allowing further facile modifications toward the potential synthesis of new drugs and supramolecular materials. The single-crystal X-ray diffraction structure of **AdBr** further confirmed the NMR, FTIR and elemental analysis results.

Supplementary Materials: The following are available online at https://www.mdpi.com/article/10.3390/org2040022/s1, A PDF file of the NMR spectra and crystal structure report for AdBr.

Funding: This research received no external funding.

Institutional Review Board Statement: Not applicable.

Informed Consent Statement: Not applicable.

Data Availability Statement: The data presented in this study are available in the Supplementary Material. Crystallographic data can be obtained free of charge via www.ccdc.cam.ac.uk/data_request/cif, or by emailing data_request@ccdc.cam.ac.uk. CCDC #: 2107042, doi:10.5517/ccdc.csd.cc28qk3p.

Acknowledgments: The author recognizes the role of Clemson University in supporting this scholarly work. Colin McMillen is credited for obtaining the crystal structure of **AdBr**.

Conflicts of Interest: The authors declare no conflict of interest.

Sample Availability: Samples of the compounds AdBr are not available from the author.

References

1. Nasrallah, H.; Hierso, J.-C. Porous Materials Based on 3-Dimensional Td -Directing Functionalized Adamantane Scaffolds and Applied as Recyclable Catalysts. *Chem. Mater.* **2019**, *31*, 619–642. [CrossRef]
2. Von Schleyer, P.R. A Simple Preparation of Adamantane. *J. Am. Chem. Soc.* **1957**, *79*, 3292. [CrossRef]
3. Schleyer, P.v.R.; Donaldson, M.M.; Nicholas, R.D.; Cupas, C. Adamantane. *Org. Synth.* **1962**, *42*, 8.
4. Davies, W.L.; Grunert, R.R.; Haff, R.F.; McGahen, J.W.; Neumayer, E.M.; Paulshock, M.; Watts, J.C.; Wood, T.R.; Hermann, E.C.; Hoffmann, C.E. Antiviral Activity of 1-Adamantanamine (Amantadine). *Science* **1964**, *144*, 862. [CrossRef]
5. Maassab, H.F.; Cochran, K.W. Rubella Virus: Inhibition in vitro by Amantadine Hydrochloride. *Science* **1964**, *145*, 1443. [CrossRef]
6. Lee, D.-W.; Jihoon Jo, J.; Jo, D.; Kim, J.; Min, J.-J.; Yange, D.H.; Hyun, H. Supramolecular assembly based on host–guest interaction between beta-cyclodextrin and adamantane for specifically targeted cancer imaging. *J. Ind. Eng. Chem.* **2018**, *57*, 37–44. [CrossRef]
7. Rodell, C.B.; Ahmed, M.S.; Garris, C.S.; Pittet, M.J.; Weissleder, R. Development of Adamantane-Conjugated TLR7/8 Agonists for Supramolecular Delivery and Cancer Immunotherapy. *Theranostics* **2019**, *9*, 8426–8436. [CrossRef]
8. Welling, D.M.; Duszenko, N.; Van Willigen, D.M.; Smits, W.K.; Buckle, T.; Roestenberg, M.; Van Leeuwen, F.W.B. Cyclodextrin/Adamantane-Mediated Targeting of Inoculated Bacteria in Mice. *Bioconjugate Chem.* **2021**, *32*, 607–614. [CrossRef] [PubMed]
9. Balzarini, J.; Orzeszko, B.; Maurin, J.K.; Orzeszko, A. Synthesis and anti-HIV studies of 2-adamantyl-substituted thiazolidin-4-ones. *Eur. J. Med. Chem.* **2007**, *42*, 993–1003. [CrossRef]
10. Ondrusek, B.A.; Chung, H. Modified *N*-Heterocyclic Carbene Ligand for the Recovery of Olefin Metathesis Catalysts via Noncovalent Host–Guest Interactions. *ACS Omega* **2017**, *2*, 3951–3957. [CrossRef]
11. Kim, C.; Ondrusek, B.A.; Chung, H. Removable Water-Soluble Olefin Metathesis Catalyst via Host–Guest Interaction. *Org. Lett.* **2018**, *20*, 736–739. [CrossRef]
12. Gupta, S.; Sabbasani, V.R.; Su, S.; Wink, D.J.; Lee, D. Alkene-Chelated Ruthenium Alkylidenes: A Missing Link to New Catalysts. *ACS Catal.* **2021**, *11*, 1977–1987. [CrossRef]
13. Wanka, L.; Iqbal, K.; Schreiner, P.R. The Lipophilic Bullet Hits the Targets: Medicinal Chemistry of Adamantane Derivatives. *Chem. Rev.* **2013**, *113*, 3516–3604. [CrossRef] [PubMed]
14. Senchyk, G.A.; Lysenko, A.B.; Krautscheid, H.; Rusanov, E.B.; Chernega, A.N.; Kraämer, K.W.; Liu, S.X.; Decurtins, S.; Domasevitch, K.V. Functionalized Adamantane Tectons Used in the Design of Mixed-Ligand Copper(II) 1,2,4-Triazolyl/Carboxylate Metal–Organic Frameworks. *Inorg. Chem.* **2013**, *52*, 863–872. [CrossRef]
15. Dsouza, R.N.; Pischel, U.; Nau, W.M. Fluorescent Dyes and Their Supramolecular Host/Guest Complexes with Macrocycles in Aqueous Solution. *Chem. Rev.* **2011**, *111*, 7941–7980. [CrossRef]
16. Granadero, D.; Bordello, J.; Pérez-lvite, M.J.; Novo, M.; Al-Soufi, W. Host-Guest Complexation Studied by Fluorescence Correlation Spectroscopy: Adamantane–Cyclodextrin Inclusion. *Int. J. Mol. Sci.* **2010**, *11*, 173. [CrossRef] [PubMed]
17. Kashani, S.K.; Jessiman, J.E.; Newman, S.G. Exploring Homogeneous Conditions for Mild Buchwald–Hartwig Amination in Batch and Flow. *Org. Process Res. Dev.* **2020**, *24*, 1948–1954. [CrossRef]

18. Fayssal, S.A.; Naret, T.; Huc, V.; Buendia, J.; Martini, C.; Schulz, E. Benzyloxycalix[8]arene supported Pd–NHC cinnamyl complexes for Buchwald–Hartwig C–N cross-couplings. *Catal. Sci. Technol.* **2021**, *11*, 5223–5231. [CrossRef]
19. Seifinoferest, B.; Tanbakouchian, A.; Larijani, B.; Mahdavi, M. Ullmann-Goldberg and Buchwald-Hartwig C−N Cross Couplings: Synthetic Methods to Pharmaceutically Potential N-Heterocycles. *Asian J. Org. Chem.* **2021**, *10*, 1319. [CrossRef]
20. Wang, X.; Zhang, Y.; Sun, X.; Bian, Y.; Ma, C.; Jiang, J. 2,3,9,10,16,17,24,25-Octakis(octyloxycarbonyl)phthalocyanines. Synthesis, Spectroscopic, and Electrochemical Characteristics. *Inorg. Chem.* **2007**, *46*, 7136–7141. [CrossRef]
21. Lie Chen, L.; Chen, Y.; Yao, K.; Zhou, W.; Li, F.; Chen, L.; Hu, R.; Tang, B.Z. Synthesis and Helical Conformation of Novel Optically Active Liquid Crystalline Poly(*p*-phenylene)s Containing Cyanoterphenyl Mesogen as Pendant. *Macromolecules* **2009**, *42*, 5053–5061. [CrossRef]
22. Medvedeva, I.V.; Stokes, M.E.; Eisinger, D.; Labrie, S.T.; Ai, J.; Trotter, M.W.B.; Schafer, P.; Yang, R. Large-scale Analyses of Disease Biomarkers and Apremilast Pharmacodynamic Effects. *Sci. Rep.* **2020**, *10*, 605–611. [CrossRef] [PubMed]
23. Alizadeh, A.; Farajpour, B.; Knedel, T.-O.; Janiak, C. Synthesis of Substituted Phthalimides *via* Ultrasound-Promoted One-Pot Multicomponent Reaction. *J. Org. Chem.* **2021**, *86*, 574–580. [CrossRef]
24. Basarić, N.; Horvat, M.; Franković, O.; Mlinarić-Majerski, K.; Jörg Neudörfl, J.; Griesbeck, A.G. Photoinduced hydrogen atom abstraction in N-(adamantyl)phthalimides: Structure–reactivity study in the solid state. *Tetrahedron* **2009**, *65*, 1438–1443. [CrossRef]
25. Wilkinson, S.M.; Barron, M.L.; O'Brien-Brown, J.; Janssen, B.; Stokes, L.; Werry, E.L.; Chishty, M.; Skarratt, K.K.; Ong, J.A.; Hibbs, D.E.; et al. Pharmacological Evaluation of Novel Bioisosteres of an Adamantanyl Benzamide $P2X_7$ Receptor Antagonist. *ACS. Chem. Neurosci.* **2017**, *8*, 2374–2380. [CrossRef] [PubMed]
26. Danopoulos, A.A.; Cole, P.; Downing, S.P.; Pugh, D. Copper and palladium complexes with *N*-heterocyclic carbene ligands functionalised with carboxylate groups. *J. Organomet. Chem.* **2008**, *693*, 3369. [CrossRef]
27. Sabbasani, V.R.; Lee, H.; Xia, Y.; Lee, D. Complementary Iron(II)-Catalyzed Oxidative Transformations of Allenes with Different Oxidants. *Angew. Chem. Int. Ed.* **2016**, *55*, 1151. [CrossRef]
28. Mack, H.; Della Vedova, C.O.; Willner, H. Structures and conformations of carbonyl and carbonyl azides. An experimental and investigation. *J. Mol. Struct.* **1993**, *291*, 197–209. [CrossRef]
29. Al-Far, R.; Ali, B.F.; Al-Sou'oud, K. Br···HN, N···HC, Br···HC, and Br···Br intermolecular interactions as supramolecular synthons: Synthesis and crystal structure of bis(2-amino-5-methylpyridinium) tetrabromomercurate(II). *J. Chem. Crystallogr.* **2006**, *36*, 523–529. [CrossRef]
30. Bolotin, D.S.; Il'in, M.V.; Suslonov, V.V.; Novikov, A.S. Symmetrical Noncovalent Interactions Br···Br Observed in Crystal Structure of Exotic Primary Peroxide. *Symmetry* **2020**, *12*, 637. [CrossRef]